Review of Satellite Remote Sensing Use in Forest Health Studies

Junming Wang[a*], Ted W. Sammis[a], and Vince P. Gutschick[b]

[a] Department of Plant and Environmental Sciences, New Mexico State University, Las Cruces, New Mexico.

[b] Biology Department, , New Mexico State University, Las Cruces, New Mexico.

* Corresponding author. Department of Plant and Environmental Sciences, Box 30003 MSC 3Q, New Mexico State University, Las Cruces, NM 88003-8003; phone: 505-646-3239; fax: 505 646- 6041; e-mail: jwang@weather.nmsu.edu.

Abstract

Satellite remote sensing has been used in forest health management by providing methods for vegetation mapping, fire fuel mapping, fire risk estimates and fire detection, post-fire severity mapping, insect-infestation mapping, and relative water stress monitoring. This paper reviews the efforts in the field of satellite remote sensing for forest health, including current research activities, the satellite sensors, methods and parameters used, and their accuracy.

The review concludes that the MODIS satellite data (Moderate Resolution Imaging Spectroradiometer) is more appropriate for most of the remote sensing applications for forest health than other current satellite data when considering temporal and spatial resolutions, cost, and bands. MODIS has a 1-2 day temporal and 250-1000m spatial resolutions, the data are free and cover more spectral bands than other satellites (up to 36 bands). Physical and physiological modeling (e.g., ET and biomass growth) should be developed for remote sensing of forest health. In addition, some satellite sensors such as for high temperature estimates (as high as 1800 K) and sensors of narrow bands are needed.

Introduction

Campbell (2002) defines remote sensing as: “the practice of deriving information about the earth’s land and water surfaces using images acquired from an overhead perspective, using electromagnetic radiation in one or more regions of the electromagnetic spectrum, reflected or emitted from the earth’s surface.” Remote sensing sensors can be instrumented on satellites, airplanes, balloons, or remote controlled vehicles.

The current and past satellite remote sensing of forest health has focused on the following categories: vegetation and landscape classification, biomass mapping, invasive plants detection, fire fuel mapping and canopy or foliar water stress, fire detection and progression mapping, post fire burn area and severity mapping, and insect infestation detection. Most of the studies have analyzed spectral signatures or simple indices (calculated from reflectance data) such as the Normalized Difference Vegetation Index (NDVI). Little has been done for remote sensing of absolute forest water stress (e.g., ET) and biomass growth using physically and physiologically based algorithms. Previous studies estimated biomass by using NDVI or other simple indices using correlation and regression methods. These studies may not result in accurate biomass growth estimates for other locations and different environmental conditions (Foody et al., 2003).

Institutes working on satellite remote sensing of forest health include: USDA Forest Service, universities, state forest service, federal institutes (e.g., NASA, NOAA, USGS, USDA ARS), private companies. Most of the studies (41%) have been conducted by USDA Forest Service, but universities represent 28% of the research in forest remote sensing (based on the paper numbers of different institutes in the proceedings of 2004 10th Biennial Forest Service Remote Sensing Applications Conference. April 2004, Salt Lake City, UT).

Satellite sensors used in remote sensing of forest health

An understanding of the satellite sensors is essential to understand the remote sensing capabilities of each satellite in terms of the type of tools that can be developed using the satellite information to make forest management decisions. Cost of the products are also a limitation in their use with management tools. There are 9 satellite sensors that are widely used in forest health research (Table 1 and 2) The major satellite sensors are ASTER (Advanced Spaceborn Thermal Emission and Reflection Radiometer), ALI (Advanced Land Imager), AVHRR (Advanced Very High Resolution Radiometer), MODIS, Landsat 5 TM (Thematic Mapper) and Landsat 7 ETM+ (Enhanced Thematic Mapper Plus), Spot 4 and 5, Quickbird-2, and IKONOS-2. Each sensor has its own advantages and disadvantages on spatial and temporal resolutions, cost, and acquisition time. The high-spatial-resolution sensors (15 m-120 m) such as ASTER, ALI, and Landsat, can not give a high temporal resolution (Their temporal resolution is more than 16 days). Furthermore, the cost of data from these sensors ranges from $80 to $600 a scene (each scene covers 25×25 km^2 to 60×60 km^2).

Although Quickbird-2, IKONOS-2, and Spot 4 and 5 have high spatial (0.61-20 m) and temporal resolutions (1-3.5 days), the temporal resolution is for future data (requested data) and the past data for an area may have not been available for the 1-3.5 day resolution, i.e., nobody requested for the data and consequently, no data was collected. In addition, the cost will be large for a forest cover scale ($15 to $22.5 per km^2 for Quickbird-2 and IKONOS-2, and $3,375-$6,750 for each Spot 5 scene of 56×56 km^2). Moreover, the satellites do not have thermal bands and consequently, can not provide data to map ET using an energy balance method (e.g., Bastiaanssen et al., 2005; French et al 2005; Kustas and Norman, 2000). MODIS data has a 1 or 2 day frequency and a 250 m to 1000 m spatial resolution. For forest health monitoring, MODIS has the necessary temporal and spatial resolutions. Also, the data are free and cover more bands than other satellites (totally 36 bands).

The satellite data is available as both raw data and processed data where the raw data is corrected for atmospheric affects and algorithms are used to produce specified products such as surface temperature. Specifically, the Landsat 5 TM and 7 ETM+ data (radiance) is about $600 a scene for the Systematic Correction (Level 1G) product. (http://edc.usgs.gov/products/satellite/landsat7.html#prices). The Systematic Correction includes radiometric correction, geometric correction, and replacement of missing image pixels. (Image correction is a crucial component for accurate information extraction and is considered a prerequisite for quality and consistency.) (http://eros.usgs.gov/products/satellite/landsat7.html#description).

The Landsat 7 ETM+ data has the highest thermal band resolution among all the current satellite sensors. The Landsat 5 TM and 7 ETM+ sensors have high resolutions in the visible, and near and short wave infrared bands. However, the data are only collected upon request because of hardware limitation (the satellite memory size is

limited for storing the high temporal resolution data) and consequently the historical data may have not been available for a location because it was not requested. The data temporal resolution of 16 days or more makes Landsat imagery acquisition sometimes problematic. It can not be used in emergency situations (e.g., fires). Even for forest water stress monitoring, the temporal resolution is a problem. In addition, the scene size is not appropriate for national mapping.

Satellite instrument problems do occur that degrade satellite products. Due to problems with the scan line corrector (SLC) on the sensor (Landsat 7 ETM+), only the middle 20 km of the imagery is currently useful. (Clark et al., 2004).

EOC (Earth Observation Center) found that the Landsat 5 TM data after July 14, 1998 could not be used for images. Because of the above circumstances, EOC decided to terminate the data reception of MSS (multiple spectral system, i.e., the non-TIP bands) data at EOC, but the MSS data acquired before that date will be still provided (http://www.eoc.jaxa.jp/whatsnew/mss_stop_e.html).

Landsat does not provide higher level products such as surface temperature, and reflectance which are important variables for water stress (ET) model based on energy balance (Bastiaanssen et al., 2005; Wang et al., 2005a). This variable must be calculated from lower level data.

In addition to Landsat 5 and 7, Landsat also launched Landsat 1 to 4 in different years (1972, 1975, 1978, and 1982). Landsat 4 had the same bands as Landsat 5 and routine collection of MSS data was terminated in late 1992 and the thermal infrared data were discontinued in August 1993 because of transmission failure. Landsat 1, 2 and 3 only had MSS data and were decommissioned in 1978, 1982 and 1983.

The ASTER sensor was launched the same year as the Landsat 7 ETM+ satellite (Table 1) but the instrumentation package was changed to record more band widths (Table 2). In addition, one more telescope is used to view backward in the near-infrared spectral band (band 3B the following) for stereoscopic capability. The ASTER data has similar applications as Landsat because it has similar bands and resolution as Landsat. All ASTER data were free before March 2006. Now each scene of both lower and higher level products (e.g., temperature, reflectance derived from raw data) is about $80. Except for Landsat 7 ETM+, ASTER data has the highest thermal band resolution among all the current satellite sensors, and it has high resolution in the visible and near infrared bands.

ASTER higher level products provide temperature and reflectance data needed as inputs into the energy balance based ET-model (Wang et al., 2005a, b) Like Landsat, the temporal resolution of 16 days or more makes ASTER data application in forest health sometimes problematic. Consequently, ASTER data are more appropriate for research purposes than operational applications.

The Spot 4 satellite sensor was launched one year before Landsat 7 ETM+ and one and half years before ASTER sensor. The Spot 5 was launched about 4 years later than Spot 4 (Table 1). The instrumentation packages of Spot 4 and 5 were different from ASTER (Table 2) and Landsat, also these satellites were owned by a private company (Space Imaging) in France and not by NASA. The spectral resolution and band width of Spot 4 and 5 are limiting (Table 2) compared to Landstat and ASTER, but the resolution is much higher. For example, Spot 5 has a 2.5-m spatial resolution for the panchromatic band and a 3-day temporal resolution compared to 15-m and 16-day for Landstat and ASTER. Spot data has been used for monitoring forest fire progression, post-fire severity mapping, invasive weed detection, and vegetation mapping (Clark et al., 2004). The biggest drawback of using Spot imagery is the high cost of the delivered data. Use of Spot 4 costs $1200-$1,900 per scene, plus additional fees for rush programming and delivery if the need is urgent (e.g., fires). RSAC (Remote Sensing Applications Center - USDA Forest Service) typically pays about $9,175 for a Spot 4 scene for BAER (Burned Area Emergency Response) support. A Spot 5 scene costs $3,300, plus additional fees for rush programming and delivery. RSAC typically pays about $10,575 for a Spot 5 scene for BAER support (Clark et al. 2004). To ensure prompt image delivery for emergency events, researchers can order Spot imagery without any terrain correction. This adds a few hours of processing time to make the imagery usable for immediate post-fire assessment but saves days of processing time at Spot Image Corporation (Clark et al. 2004). Spot does not have thermal infrared bands and can not provide surface temperature products for ground heat mapping or the calculation of ET based on energy balance.

Several AVHRR sensors have been launched since June 11, 1978 providing continuous historical to present data. The temporal resolution is daily with the spectral resolution of 4 to 5 bands. The spatial resolution is 1100 m. This sensor is owned by NOAA/NASA. This sensor has fewer spectral bands than Landsat 5 and 7, ASTER, ALI, and MODIS. AVHRR's objective is to provide radiance data for investigation of clouds, land-water boundaries, snow and ice extent, ice or snow melt inception, day and night cloud distribution, temperatures of radiating surfaces, and sea surface temperature. Other applications include agricultural assessment, land cover mapping, fire and burnt area mapping, production of large-area maps, and evaluation of regional and continental snow cover

(http://gcmd.nasa.gov/KeywordSearch/Metadata.do?Portal=GCMD&KeywordPath=&EntryId=AVHRR&MetadataView=Full&MetadataType=0). The AVHRR raw data (not geo-registered) are free. However, dates are provided only in limited sets. The geo-registered raw data is $190 a scene. (http://edc.usgs.gov/products/satellite/avhrr.html). The AVHHR data include thermal infrared data but not derived temperature data that can be used to estimate ET (energy balance based) (Wang et al., 2005 a, b). The disadvantage to using AVHHR imagery is the coarse spatial resolution, which often is too coarse for fire analysis (Clark et al. 2004).

There are two MODIS sensors. One is on Terra satellite which carries the ASTER sensor also. The other MODIS sensor is on Aqua satellite. Although Terra ASTER and MODIS are on the same satellite, the temporal resolution of this MODIS is much shorter than ASTER's (1 day vs.16 days) because MODIS view field is much larger than ASTER's (2300×2300 km^2 vs. 60×60 km^2). Terra MODIS and ASTER were launched by NASA in the same year as Landdsat 7 ETM+ (Table 1) but the MODIS spatial resolution was coarse. The MODIS sensors' temporal resolution is daily with the spectral resolution of 36 bands (Table 1 and 2). Currently, MODIS data are free. MODIS data have been used in monitoring forest fire, post-fire burn area mapping, vegetation classification, biomass estimation, and soil degradation

Because the first seven bands of MODIS were designed to simulate the Landsat sensor except for the spatial resolution, users can view MODIS imagery much the same way as Landsat imagery (Clark et al. 2004). MODIS also, provides products of surface temperature, reflectance which drive ET model (energy balance based) (Wang et al., 2005 a, b). Like AVHHR data, the disadvantage to using MODIS imagery is the coarse spatial resolution. The finest pixel size is 250 meters, which often is too coarse for fire analysis (Clark et al. 2004).

NASA launched the Advanced Land Imager (ALI) in November 2000 (Table 1) to supplement data from Landsat. Because ALI follows the same orbit track as Landsat 7, images can be acquired from this satellite in addition to Landsat 7 to get better temporal resolution.

The ALI is an experimental sensor and provides Landsat-type panchromatic and multi-spectral bands. Consequently, the data applications are similar to those for Landsat. The bands have been designed to mimic six Landsat MSS bands with three additional bands covering 0.433-0.453 μm, 0.845-0.890 μm, and 1.20-1.30 μm (Table 2). In theory, this sensor could be a replacement for Landsat 7 (Clark, 2004). Archived ALI radiometrically corrected data are $250 a scene; Archived radiometrically and geometrically corrected data are $500 a scene. Data Acquisition Requests (DARs) must be submitted in order to collect a requested image for a specific area of interest. There will be a $750 service fee for tasking the sensor(s) (http://eo1.usgs.gov/products.php).

Because this sensor is still experimental, NASA does not acquire the full 185 kilometer by 185 kilometer footprint. ALI images are much more narrow than a typical Landsat footprint. For example, the image acquired of the Old/Grand Prix fires was only 37 kilometers wide and 185 kilometers in length (Clark et al. 2004). The ALI sensor does not have any thermal bands.

Quickbird-2, owned by one of three private satellite companies offering remote sensing information for profit, was launched by DigitalGlobe Corporate in the U.S. in

2001 with high spatial and temporal resolutions (Table 1 and Table 2). Quickbird-2 has the highest spatial resolution in panchromatic, visible, and near infrared bands among the satellite sensors. The data are used for vegetation classification, invasive weed detection, insect-infested mapping, landscape classification, and forest fire fuel mapping. It is $22.5 for 1 km^2 for the archived data, minimum 25 km^2. New data acquisition requests have a minimum requirement of 64 km^2. Because it has no thermal bands, surface temperature data can not be estimated and provided. Scene size is relatively small and may not be large enough for forest mapping. Costs also limit its use for forest health monitoring.

IKONOS-2 was launched in 1999 by a private company (Space Imaging) in France. Like Quickbird-2, IKONOS-2 collects high spatial resolution data (Table 1 and 2). It is $7 for 1 km^2 for the archived data, minimum 49 km^2 and new data (Data Acquisition Requests) are $15 for 1 km^2, minimum 100 km^2. Except for the Quickbird-2, IKONOS-2 has the highest spatial resolution in the panchromatic, visible, and near infrared bands among the satellite sensors (Table 2). Consequently, IKONOS-2 data are used for vegetation classification, landscape classification, and burn area mapping. Similar to Quickbird-2, it has no thermal bands which can be used for surface temperature estimation.

Data formats and software tools to view the data

The common used satellite data formats are HDF (Hierarchical Data Format) and GeoTIFF (Geographic Tagged Image File Format). Data from NASA usually have these formats (Table 5). Some early satellites from NASA like AVHRR and Landsat have other data formats: Fast, NDF, and NITF. NDF represents the National Landsat Archive Production System Data Format (NLAPS Data Format) (http://landsat.usgs.gov/data_products/product_information.php). NITF is National Imagery Transmission Format. Spot satellites from the French company have special formats: CAP and DIMAP. One format is called the "CAP format", since it has been designed to be produced by the Centred'Archivage et de Prétraitement (CAP) located at SPOT IMAGE premices. DIMAP, which stands for Digital Image Map, is the new SPOT product data format introduced in mid-2002 for the launch of the new SPOT 5 satellite.

All the above data formats need special reader software to open and view. Most of them are proprietary (Table 5). ENVI software can read all the satellite data formats mentioned. The price for ENVI Windows version is about $1250 for educational institute and $5000 for commercial institutes (https://www.ittvis.com/pricing).

There are also some free software packages (Table 5). For example, HDFview is from NASA which is a user-friendly software package and can read HDF files (http://www.hdfgroup.org/hdf-java-html/hdfview/). The source codes are in JAVA and can be downloaded for free.

If some researchers or other users want to program their own software to read satellite data, it will need much effort. For example, we tried to program a MODIS (L1 B 1000 m) raw data reader. MODIS raw data (L1 B 1000 m) have the HDF format. However, the data inside the files can also have different formats. Some of the files contain compressed data format inside the files and other may just contain the uncompressed data.

Indices and data transformations used in remote sensing of forest health

An index is formed from combinations of several spectral values from satellite data that are added, divided, or multiplied in a manner designed to yield a single value (Campbell, 2002). In satellite remote sensing for forest health, the indices of vegetation, burn and foliar moisture, and data transformations are often used as the preprocessed data for regression or other data analysis. Regression analysis between an index and a physical characteristic in the forest is a first approximation of the physical characteristic observed by the satellite data. Consequently, regression analysis have low coefficient of determination when using indices to predict plants response to a changing environment and future work need to be based on the physiology of the plants response to its environment as observed by the satellite such as the surface temperature response of plants to moisture stress. However indices and regression analysis still result in valuable information.

Plants absorb red light by chlorophyll and strongly reflect infrared radiation by mesophyll tissue. Thus, infrared reflectance will be high and red reflectance will be low for actively growing plants. Infrared and red reflectances are commonly used in vegetation indices (Campbell, 2002). Researchers have proposed a number of spectral vegetation indices premised on the contrasts in spectral reflectance between green vegetation and background materials (Rouse et al. 1974; Richardson and Wiegand, 1977; Tucker, 1979; Jackson, 1983). Of the indices, Normalized Difference Vegetation Index (NDVI, Rouse et al., 1974) is the most commonly utilized which is based on infrared and red reflectances (Table 3). NDVI has been used for fuel mapping, foliar moisture stress detection, burn severity mapping, vegetation classification, forest type mapping, invasive weed detection, and land degradation model (Table 4).

Foliar moisture indices indicate leaf moisture. Because plant leaf moisture is related to short wave infrared band (Toomey and Vierling, 2005), foliar moisture indices are formulated with the short wave infrared band and other bands (Table 5).

Burn indices, detecting burnt and burning areas, are usually formulated with near infrared and short wave bands. These two bands exhibited the greatest reflectance change in response to fire. Short wave reflectance increases with fire, while near infrared decreases (Key and Benson, 2002). The commonly used burn index is the Normalized Burn Ratio (NBR, Table 5) which is widely used in burning detection and burn severity mapping (Table 6).

Data Transformations

Because of the low coefficient of variation between an satellite derived index and a measured physical characteristic on the ground, two data transformations methods are often used in remote sensing of forest health, the Principal Component Analysis (PCA) and Tasseled Cap Transformation (TCT). PCA is a classical statistical method equivalent to transforming the data to a new coordinate system with a new set of orthogonal axes, which reduces the information of the reflective bands into fewer useful vectors (i.e, eigenvectors, a mathematical term) which explain the majority of the variation (Rollins et al., 2005). The TCT, which is mathematically similar to the PCA but data independent (Kauth and Thomas 1976; Crist et al., 1986) and based on

empirical observations, was performed on all images. TCT gets three major physical bands, wetness, brightness, and greenness. The actual details had a more analytical basis (Toomey and Vierling 2005).

Fire fuel mapping

The type, composition, and distribution of fuels (Chuvieco and Congalton, 1989) are the most important factors influencing fire hazard and fire risk. Wildland fuels are typically divided into three strata: ground fuels, surface fuels, and crown fuels (Pyne et al., 1996). Remote sensing based fuels mapping has typically employed one of the Landsat sensors (TM, or ETM+) to map fuels characteristics (Riano et al., 2003) (Table 4). Quickbird-2 and ASTER satellite have also been used for fuel mapping (Falkowski et al., 2005).

The common methods used in fuel mapping are regression methods and gradient modeling (Falkowski et al., 2005; Rollins et al., 2005; Keane et al., 2002; Kessell, 1979). Gradient modeling refers to the use of environmental gradients (topographical, biogeochemical, biophysical, and vegetational) to model the occurrence of natural phenomena (Keane *et al.*, 2002). This approach has been used with moderate success in estimating fuel types and fuel loading. Environmental gradients such as topography, moisture, and time since last burn have a large impact on fuel loading (Kessell, 1979). High fuel loading, for example, can be partially explained by lower decomposition rates (characterized by moisture and temperature gradients) and a long time interval since the last fire (Keane et al., 2001).

The input parameters derived from satellite data for regression equations or gradient models are vegetation indices (Table 3 and 4) and spectral transformations such as PCA and TCT. The outputs of fuel mapping usually are fuel load (kg/m^2), canopy closure (percent cover), bulk density, canopy height, and vegetation types. The accuracy is around 50% to 85% even after using PCA or TCT analysis.

Foliar moisture stress detection

Foliar moisture stress is mapped for fire risk assessment. The so-called foliar moisture stress, or SMC (mass of foliar water per unit area) is defined as the total understory and overstory leaf moisture per unit area (kg H_2O /m^2) (Toomey and Vierling, 2005). Landsat, ASTER, and Spot have been used for foliar moisture prediction. Regression methods are the commonly used methods (Tucker, 1980; Hunt and Rock, 1989; Downing et al., 1993; Chuvieco et al. 1999; Serrano et al., 2000; Ceccato et al., 2001; Ceccato et al., 2002 a, b; Toomey and Vierling, 2005). The inputs were the components of TCT, PCA, vegetation indices, or foliar moisture indices (Table 3 and 4). The R^2 values range from 0.5 to 0.8.

PCA is functional only for single-date analyses of foliar moisture, and could not be used for monitoring of forests health. Consequently, for periodic analysis and comparison, the wNDII or TCT wetness is the most suitable approach for estimating SMC (Toomey and Vierling, 2005).

Fire detection

Generally, the fire detection algorithms have three categories: single channel threshold algorithm, multiple channel threshold algorithm (Arino and Melinotte, 1998; Kennedy et al., 1994), and contextual algorithm (Flasse and Ceccato, 1996; Justice et al., 1996; Kaufman et al., 1990; Kaufman et al., 1998; Giglio, et al., 1999; Giglio et

al., 2003). Single channel threshold algorithm sets a threshold value for a band (a channel) and compares it with the measured value of the channel to determine if any fire is occurring. Multiple channel threshold algorithm sets threshold values for some indices (such as NBR) derived from values of multiple channels (multiple bands). Most of the threshold algorithms used NBR, 4 μm or 11 μm bands (Li et al., 2005).

The contextual methods were developed to be more flexible by computing variable, pixel-specific thresholds that can vary across an image instead of relying on fixed thresholds, thereby avoiding some human intervention, such as the MODIS fire detection algorithm (Giglio et al., 2003). But the MODIS fire detection is also prone to generate more false alarms. On the other hand, most contextual fire detection algorithms are complicated and a slight tuning of the algorithm may cause it to work differently (Li et al., 2005).

Besides these, there are some other kinds of fire detection algorithms, such as the MODVOLC algorithm (Wright et al., 2002). The MODVOLC algorithm utilizes the Normalized Thermal Index (NTI) (Table 3) to identify hot pixels. Each algorithm has its own strengths and limitations. For example, the MODVOLC algorithm has the strength of speed and simplicity. The weakness of the algorithm is that the algorithm needs manual tuning of the threshold to achieve high detection probability, and it tends to miss small fires. The contextual algorithms are more versatile for application to a wide range of conditions than the fixed threshold approaches (Li et al., 2005).

Li et al., (2005) developed a hybrid algorithm based on the above algorithms. The hybrid algorithm takes advantage of the strong points of each algorithm and circumvents the weaknesses to maintain high discrimination capabilities, adaptability to different geographic areas and observation conditions, and relatively simple mathematics. The algorithm was tested using MODIS images. The results display that the new algorithm has a high detection probability and low false alarm rate. The parameters used in this algorithm are listed in Table 6.

There are problems to detect fires if the algorithms only use coarse-resolution data such as MODIS or only use fine-resolution data such as Landsat or Quickbird-2. Coarse data will not detect the small fires. However, the fine-resolution data coverage is small (Kaufman *et al.,* 1990). The combination of these two kinds of data may solve theses problems.

In addition to the above problems, satellite sensors saturate at certain temperatures. For example, for MODIS sensors, the commonly used bands for fire detection are 1.65 μm (saturation temperature=740 K), 2.13 μm (saturation temperature=570 K), 4 μm (saturation temperature=500 K), and 11 μm (saturation temperature=400 K) (Kaufman and Justice, 1998). However, the fire temperature can be as high as 1800 K (Boyd and Danson, 2005) which may result in sterilized (infertile) soil and the post-fire vegetation recovery will be difficult. The sensor and algorithm for estimating high temperatures need to be developed in order to estimate fire damage more precisely.

Post-fire burned area mapping

After forest fires, the burn area and burn severity need to be mapped to help rehabilitation. The commonly used parameters for estimates of burn severity and area are NBR, dNBR, NDVI (Table 5). Usually, researchers use the indices (NBR , NDVI, dNBR) with a threshold value or a regression equation to predict the burn area and burn severity (high, moderate, low and unburned classes) (Salvador et al., 2000; Fraser and Li, 2002; Hudak et al., 2004a, b; Cocke et al., 2005, Table 6). In addition,

some researchers observe temporal differencing of spectral transform (TCT) to detect the burned area (Rogan and Yool, 2001; Lieberman et al., 2004).

Lieberman (2004) examined the use of satellite multi-spectral imagery to map three-levels of fire severity within two southern California fire scars. They compared the effects of spectral transforms, temporal dimensionality, classifiers, and satellite sensor types on the ability to accurately map wildfire severity when field data was used for training. Temporal differencing of the TCT on Landsat Thematic Mapper (TM) imagery was the most accurate of all approaches and image type tested for both burn sites. The classification maps derived from NBR, spectral transform on TM imagery and nonenhanced IKONOS-2 multi-spectral image resulted in the lowest accuracies.

Mapping of vegetation, landscape, insect infestation, and invasive weeds

Vegetation and landscape mapping (including insect infestation and invasive weed mapping that were vegetation mapping also) used image segmentation (classification) algorithms. There are two general types of classification algorithms: unsupervised and supervised (Brown et al., 1993; Jensen, 1996; Saatchi and Rignot, 1997; Steininger et al., 2001; Foody, 2002; Campbell 2002; Hoppus and Lister, 2005). In supervised classification, known spectral reflectance values either derived from known locations on the image or handheld spectrometers are used to identify other pixels having the same reflection. In unsupervised classification algorithms, a computer recognizes different patterns and classifies them to different vegetation or land cover. In general, supervised classifications are more accurate than unsupervised. The classification software packages of eCognition (Definiens Inc., Boston, MA, USA), Feature Analyst (Visual Learning System, Inc., Missoula, MT), ERDAS Imagine (Geosystems Geospatial Imaging, LLC, Norcross, GA, USA) have been commonly used for vegetation classification and mapping (Ruefenacht, 2004**)**.

Regression-tree classification is a relatively new procedure for land cover classification. Regression-tree classification procedures have several advantages over more traditional classification procedures such as supervised and unsupervised algorithms. Regression-trees are non-parametric and, as such, do not require knowledge about data distributions and can handle non-linear relationships between variables. They can also allow for missing data values, handle both numerical and categorical data, and incorporate multiple remote sensing and GIS data layers. Regression-tree classifications are significantly less labor intensive than other classification techniques and can be used efficiently for large land cover classifications. Accuracies of regression-tree classifications are either similar to or better than supervised/unsupervised classification (Ruefenacht, 2004).

For the mapping of vegetation, landscape, insect infestation, and invasive weeds, the input data from satellite usually are NDVI, EVI, MSAVI, TCT brightness, greenness, and wetness, elevation, aspect, and slope. The outputs are percent canopy cover, forest/nonforest classification, tree types (Table 4). The accuracy was from 50% to 99%. The accuracy depends on the predictor variable selection and dependent variable type. For example, the forest/nonforest classification (dependent variable) obtained the highest accuracy than other types of classifications such as classifying different tree types.

Forest vigor

Cost effective methods are necessary for broad-scale regular assessment of forest vigor over complex terrain. Satellite derived vegetation indices such as NDVI can monitor large remote areas with an effective database for evaluating vegetation vigor. High percentages of spectral variance of individual scenes can be explained using TCT (Huang, et al., 2000). The TCT greenness and wetness bands have strong correlation to the percentage of vegetation cover (Crist *et al*., 1986). The greenness feature measures the presence and density of green vegetation while the wetness feature measures soil moisture content and vegetation density (Crist et al., 1986).

For example, Beck and Gessler (2004) proposed methods for mapping and monitoring forest status through the creation of departure maps from average NDVI, TCT greenness, and wetness index derived from an expanding time-series of Landsat imagery. Methods for displaying negative and positive departures was presented and evaluated for significance in support of forestland management. Current departure classification clearly delineates major disturbances such as roads and forest harvest activities within the negative departure from average class.

Stand volume and biomass

Compared with vegetation classification (e.g., percent canopy cover), forest stand volume and biomass estimation were less accurate (Table 4, Foody et al., 2003; Moisen et al., 2004; Falkowski et al., 2005; Lu, 2006). The R^2 is usually below 50%. The commonly used methods are regression using vegetation indices as the inputs. The low accuracy may be from the weak relationship between the dependent variables (biomass and volume) and the predictor variables (e.g, NDVI).

Biomass estimation was also used in rangeland management. For example, Gillham and Mellin (2004) conducted temporal image analysis to assist rangeland managers in assessing range readiness, monitoring utilization levels, and making decisions to extend or shorten the length of the grazing season. Landsat TM and ETM+ images were used to develop correlations between the field gathered data (dry biomass weight per unit area) and remotely sensed imagery. Overall R^2 was 0.68. MODIS satellite images were used to develop a series of greenness indices throughout the growing season but were not directly correlated with field data.

Forest ET and carbon fluxes

Forest water stress, biomass and growth (fuel level, forest vigor) are highly related to fire and insect risks. However, there have been few studies on forest ET (forest water stress indicator) and biomass growth prediction. Previous studies estimated forest water stress (foliar moisture) using regression equations from inputs of vegetation and moisture indices or PCA and TCT transformed data (Ceccato et al., 2002 a ,b; Toomey and Vierling, 2005). Regression equations may produce errors for different locations and environmental conditions. Physically and physiologically based models need to be developed for the water stress calculation. ET models using energy balance principle for agriculture field (level-ground) are available with high accuracy) (Bastiaanssen et al., 1998; Courault et al., 2003; Bastiaanssen et al., 2005; Wang et al., 2005a). The typical accuracy at field scale is 85% for 1 day and it increases to 95% on a seasonal basis (Bastiaanssen et al., 2005). Physiological relationship between ET and biomass growth was obtained from physiological models (Gutschick 2006). Therefore, the biomass growth can be calculated from modeled ET.

The difficulty in mapping forest ET and biomass growth is to correct the effects

from mountain elevation, slope, and aspect which cause surface temperature and radiation variations and can result in errors of ET estimations using energy balance methods (Morse et al., 2005; Wang et al., 2005b). Morse et al., (2005) tried to correct surface temperature effect assuming a 6.5°C /km lapse rate. However, this lapse rate is for air temperature which may not be the lapse rate for the surface temperature. Further work (experiments and models) are needed to calibrate and validate elevation, aspect, and slope effects on ET calculation.

Data management tools

There were studies focusing on the data management for the satellite remote sensing of forest health (e.g., van Leeuwen et al., 2004). The purpose is to let users more conveniently and quickly to find the desired data and obtain them. Most of these tools are web-based.

For example, the FSGeodata Clearinghouse at USDA Forest Service (http://svinetfc4.fs.fed.us/) provides searching, viewing and downloading of geospatial datasets and metadata created and maintained by the USDA Forest Service over lands in the National Forest System. Access to datasets is provided through a user-driven geographic interface. It provides geospatial data, National Forest Lands Cartographic Feature Files, National Forest Lands Raster 1:24000 Map Files, and real-time and near real-time MODIS fire detection GIS data, MODIS fire detection maps, MODIS imagery, and other related fire geospatial data for the United States and Canada. The following is a sample MODIS Active Fire Detection map for southwestern US on June 9, 2006.

USGS (http://firedata.cr.usgs.gov/) also provides Internet-based fire data ordering system for use in wildfire applications for Geographical Information System technical specialists, infrared interpreters, and fire managers. The application at USGS allows for interactive display of maps integrated with current wildfire information and is enhanced with the capability to process, reproject, mosaic, and tone balance Digital Raster Graphics, Digital Orthophoto Quads, Digital Elevation Models, and automatically disseminate the data for users to download or to initiate delivery of data on CD-ROM using various mail delivery methods.

In addition, Goddard Space Flight Center and the University of Maryland built a web-based real-time automated global fire-detection system using MODIS products (http://maps.geog.umd.edu/default.asp) and the Cooperative Institute for Meteorological Satellite Studies (CIMSS) at the University of Wisconsin - Madison has used the Geostationary Satellite (GOES) series of satellites to monitor fires and smoke in the Western Hemisphere (http://cimss.ssec.wisc.edu/goes/burn/wfabba.html).

USDA Forest Service provides Forest Inventory and Analysis (FIA) data or forest resource data are used to monitor tree growth and harvests, but also tree species and land use patterns, forested wildlife habitat, mortality and other forest health attributes, regional biological processes, timber and nontimber forest products, and associated human activities. These provided data files are compressed, comma separated, and can be easily uploaded into spreadsheets.

Arizona Remote Sensing Center, Office of Arid Lands Studies, University of Arizona (http://rangeview.arizona.edu) provides a web based geospatial application for viewing, animating, and analyzing multitemporal satellite and precipitation data to permit monitoring of vegetation dynamics through time and across landscapes.

RangeView has been developed for natural resource managers but also has significant value for educators and researchers. MODIS (Moderate Resolution Imaging Spectroradiometer) derived products have been developed and integrated to facilitate monitoring and interpretation of vegetation growth, drought and wildfire dynamics. The MODIS derived products include spectral vegetation indices (250m and 1km resolution) and a prototype of associated cloud and snow cover data. A color composite image is also provided to help assess the quality of the NDVI (Normalized Difference Vegetation Index) data. The MODIS derived Leaf Area Index is provided as an additional indicator of live vegetation. The following pictures show the western US MODIS LAI (m^2/m^2) maps in January, February, March, and April of 2006.

The Pacific Northwest Region, USDA Forest Service, developed a toolkit of terrestrial ecological unit inventories (TEUI-Geospatial Toolkit) (Ufnar et al., 2004). A primary objective of the TEUI-Geospatial Toolkit is to implement national inventory protocol and provide an efficient and repeatable method for conducting TEUI at the landscape and land unit scale. The toolkit combines geospatial data preparation, visualization, on screen digitization, map unit analysis, and field-sheet map production tools in a step-by-step and user-friendly format. Using the TEUI Geospatial Toolkit, a resource specialist controls the entire mapping process from data loading to concept development to landscape stratification and validated on the ground. The tool was field verified and found to be very effective for predicting soil patterns and distribution across the study area.

The above illuminates the major operational tools for satellite remote sensing of forest health. Most of the other studies mentioned in this paper have not provided operational tools for forest health managers.

Other studies

There have been some studies in land degradation modeling and hydrology studies. For example, van Leeuwen and Sammons (2003) used MODIS products and data integration methods to assess land degradation and rehabilitation and to incorporate seasonal and geospatial vegetation and climate products into two soil erosion assessment models. The RUSLE model (Revised Universal Soil Loss Equation) was used to assess monthly soil loss. MODIS based NDVI was used to derive monthly vegetation cover and vegetation resistance to soil erosion. No ground truth comparison was conducted in this study.

Future work

Sensors

The current satellite sensor capabilities are impressive, yet some additional sensors are needed. For example, current satellite TIR sensors saturate at low fire temperatures and therefore cannot distinguish the very high-fire-temperature fires from lower temperature fires, which is important to estimate fire damage and post-fire vegetation recovery.

Several indicators of the physiological state of vegetation require narrow bandwidths (5 nm or less) that are not measured by current satellite sensors. The following illustrate some narrow-band satellite sensors that are not available.

For example, the narrow bands of green wavelength can be used to directly calculate carbon flux using the photochemical reflectance index,

$(\alpha_{531}-\alpha_{570})/(\alpha_{531}+\alpha_{570})$, where $\alpha_{531 \text{ and } 570}$ are the reflectances of narrow bands with wavelengths 531 nm and 570 nm. The index exhibits a high correlation to ground measurements via gas exchange on leaves or via flux towers (Gamon et al., 1997; Guo and Trotter, 2004; Drolet et al., 2005).

Another example is for the water index, particularly $\alpha_{900}/\alpha_{970}$, where $\alpha_{900 \text{ and } 970}$ are the reflectances of narrow bands with wavelength 900 nm and 970 nm. The index effectively measures column density of water in canopy leaves (Sims and Gamon, 2003).

One more example is the chlorophyll indices. The indices originally posited as $(\alpha_{750} - \alpha_{705}) / (\alpha_{750} + \alpha_{705})$, where $\alpha_{750 \text{ and } 705}$ are the reflectances of narrow bands with wavelength 750 nm and 705 nm, have been refined to achieve high fidelity to actual chlorophyll content, which then can be related to biomass growth (Dash and Curran, 2004).

Physical models for biophysical attributes

The limitations to inferring forest biomass, stress, water use and other attributes have been noted earlier. For example, because forest water stress strongly affects forest health which can increase the risk of fires and insect outbreak, work was done to monitor forest water stress using NDVI and other indices. However, regression equations only using these indices may not be accurate for other locations and environmental conditions.

Physical models are needed. ET is an indicator of forest water stress and may be estimated using satellite remote sensing using a physical model (e.g., energy balance model) (Wang et al, 2005b; Bastiaanssen et al., 2005; French et al., 2005; Kustas and Norman, 2000). Because the remote sensing model of level-field ET is available, the major work to adapt it to the forest will be to add the effects of the elevation, aspect, and slope of mountain areas.

As another example, a physical method needs to be developed to predict biomass growth. There was some work on forest biomass or growth estimation, which is related to fire fuel mapping. NDVI and other vegetation indices were used to predict the biomass and growth using regression equations. These equation accuracy will be affected by environmental factors, especially illuminations. A more stable method needs to be developed to predict biomass growth. Because biomass growth is highly related to ET, biomass growth can be estimated using appropriate adjustments from an ET map obtained from remote sensing (Gutschick, 2006).

Data management tools

Most forest management tools are user friendly. However, some tools require operators who are expert-level researchers. These tools are not appropriate for forest managers. Some tools require the user to operate different software packages step by step to obtain the results. In addition, some forest health tools on the Internet provide only maps, with no grid data available. The above needs to be improved in the future.

Conclusions

Current and previous satellite remote sensing of forest health have focused on the following categories: vegetation and landscape classification, biomass mapping, invasive plants detection, fire fuel mapping and canopy or foliar water stress, fire

detection and progression mapping, post-fire burn area and severity mapping, and insect infestation detection. The USDA Forest Service is the lead agency in forest status and health studies using satellite remote sensing. The major satellite sensors used for remote sensing of forest health are ASTER, ALI, MODIS, Landsat 5 TM and Landsat 7 ETM+, Spot 4 and 5, Quickbird-2, and IKONOS-2. The majority of the studies have analyzed spectral signatures or simple indices (calculated from reflectance data) such as NDVI. Correlation and regression methods are the commonly used research methods.

Among the satellite sensors, MODIS data are more appropriate for most of the remote sensing applications for forest health than other satellite data considering temporal and spatial resolutions, cost and bands. MODIS has the 1-2 day temporal and 250-1000m spatial resolutions, the data are free and cover more bands than other satellites (36 bands total).

Physical and physiological modeling (e.g., ET and biomass growth)should be developed for remote sensing of forest health. In addition, some satellite sensors such as for high temperature estimates (as high as 1800 K) and sensors of narrow bands are needed.

References:

Arino, O. and Melinotte, J.M. 1998. The 1993 Africa fire map. Int. J. Remote Sensing, 19:2019-2023.

Bastiaanssen, W.G.M., Menenti, M., Feddes, R.A., and Holtslag, A.A.M. 1998. A remote sensing surface energy balance algorithm for land (SEBAL). 1. Formulation. J. Hydrol. 212/213:198-212.

Bastiaanssen, W.G.M., Noordman, E.J.M., Pelgrum, H., Davids, G., Thoreson, B.P., and Allen, R.G. 2005. SEBAL model with remotely sensed data to improve water-resources management under actual field conditions. J. Irr. and Dra. Engr., 131:85-93.

Beck, R.N., Gessler, P.E.. 2004 Forest Vigor Assessment of the Inland Northwest using Landsat Timeseries. Proceedings of the 2004 10th Biennial Forest Service Remote Sensing Applications Conference. April 2004. Salt Lake City, UT.

Boyd, D.S., and Danson, F.M. 2005. Satellite remote sensing of forest resources: three decades of research development. Progress in Physical Geography 29, 1 (2005) pp. 1–26.

Brown, S.A., Hall, C.A.S., Knabe, W., Raich, J., Trexler, M.C. and Woomer, P. 1993: Tropical forests, their past, present and potential future role in the terrestrial carbon budget. Water, Air and Soil Pollution 70, 71–94.

Campbell, J.B. 2002. Introduction to remote sensing. New York: The Guilford Press.

Ceccato, P., Flasse, S., Tarantola, S., Jacquemoud, S., and Grégoire, J.-M. 2001. Detection vegetation leaf water content using reflectance in the optical domain. Remote Sensing of Environment, 77, 22–23

Ceccato, P., Gobron, N., Flasse, S., Pinty, B., and Tarantola, S. 2002a. Designing a spectral index to estimate vegetation water content from remote sensing data. Part 1. Theoretical approach. Remote Sens. Environ. 82: 188–197.

Ceccato, P., Flasse, S., and Gregoire, J.M. 2002b. Designing a spectral index to estimate vegetation water content from remote sensing data. Part 2. Validation and applications. Remote Sens. Environ. 82: 198–207.

Chuvieco, E. and Congalton, R.G. 1989. Application of remote sensing and geographic information systems to forest fire hazard mapping. Remote Sensing of Environment. 29:147-159.

Clark, J., Zajkowski, T., and Lannom, K. 2004. Remote sensing imagery support for burned area emergency response teams on 2003 southern California wildfires. Proceedings of the 2004 10th Biennial Forest Service Remote Sensing Applications Conference. April 2004. Salt Lake City, UT.

Cocke, A.E., Fulé, P.Z., and Crouse, J.E. 2005. Comparison of burn severity assessments using Differenced Normalized Burn Ratio and ground data. International Journal of Wildland Fire.14, 189-198.

Courault, D., Seguin, B., and Olioso, A. 2003. Review to estimate evapotranspiration from remote sensing data: some examples from the simplified relationship to the use of mesoscale atmospheric models. ICID workshop on remote sensing of ET for large regions, 17th September, 2003.

Crist, E. P., Laurin, R., and Cicone, R.C. 1986. Vegetation and soils information contained in transformed Thematic Mapper data. Proceedings of IGARSS' 1986 Symposium, Zurich, Switzerland, 8-11 September.

Dash, J., and Curran, P. J. 2004. The MERIS terrestrial chlorophyll index. International Journal of Remote Sensing 25: 5403-5413.

Downing, H.G., Carter, G.A., Holladay, K.., and Cibula, W.G. 1993.
The radiative-equivalent water thickness of leaves. Remote Sensing of Environment, 46, 103– 107.

Drake, S., Rodriguez-Gallegos, H., and Hubbard, A. 2004. Supermaps from high spatial resolution satellite imagery for vegetation mapping and monitoring. Proceedings of the 2004 10th Biennial Forest Service Remote Sensing Applications Conference. April 2004. Salt Lake City, UT.

Drolet, G. G., Huemmrich, K. F., Hall, F. G., Middleton, E. M., Black, T. A., Barr, A. G., and Margolis, H. A. 2005. A MODIS-derived photochemical reflectance index to detect inter-annual variations in the photosynthetic light-use efficiency of a boreal deciduous forest. Remote Sensing of Environment 98: 212-224.

Falkowski, M.J., Gessler, P.E., Morgan, P., Hudak, A.T., and Smith, A.M.S. 2005. Characterizing and mapping forest fire fuels using ASTER imagery and gradient modeling. Forest Ecology and Management, Volume 217, Issue 2-3, 1, pp. 129-146.

Flasse, S.P. and Ceccato, P. 1996. A contextual algorithm for AVHRR fire detection. Int. J. Remote Sensing, 17:419-424.

Foody, G.M. 2002: Status of land cover classification accuracy assessment. Remote Sensing of Environment 80, 185–201.

Foody, G.M., Boyd, D.S. and Cutler, M.E.J. 2003. Predictive relations of tropical forest biomass from Landsat TM data and their transferability between regions. Remote Sensing of Environment, 85, 463–474.

Fraser, R.H. and Li, Z. 2002: Estimating fire-related parameters in boreal forest using SPOT VEGETATION. Remote Sensing of Environment 82, 95–110.

French, A. N., Jacob, F., Anderson, M. C., Kustas, W. P., Timmermans, W., Gieske, A., Su, Z., Suf, H., McCabe, M. F., Prueger, J., and Brunsell, N. 2005.. Surface energy fluxes with the Advanced Spaceborne Thermal Emission and Reflection radiometer (ASTER) at the Iowa 2002 SMACEX site (USA). Remote Sensing of Environment 99: 55-65.

Gamon, J. A., Serrano, L., and Surfus, J. S. 1997. The photochemical reflectance index: an optical indicator of photosynthetic radiation use efficiency across species, functional types, and nutrient levels. Oecologia 112: 492-501.

Giglio, L., Descloitres, J., Justice, C.O., and Kaufman, Y. J. 2003. An enhanced contextual fire detection algorithm for MODIS. Remote Sensing of Environment, 87:273-282.

Giglio, L., Kendall, J.D., & Justice, C.O. 1999. Evaluation of global fire detection algorithms using simulated AVHRR infrared data. International. Journal of Remote Sensing, 20, 1947– 1985.

Gillham, J., and Mellin, T.C. 2004. Monitoring rangeland trends using remote sensing. Proceedings of the 2004 10th Biennial Forest Service Remote Sensing Applications Conference. April 2004. Salt Lake City, UT.

Guo, J. M., and Trotter, C. M. 2004. Estimating photosynthetic light-use efficiency using the photochemical reflectance index: variations among species. Functional Plant Biology 31: 255-265.

Gutschick, V.P., 2006. Plant acclimation to elevated CO2 - from simple regularities to biogeographic chaos. Ecol. Model. In press.

Hoppus, M.L., and Lister, A.J. 2004. How does modis imagery correlate with usda-forest service forest inventory plot data? Proceedings of the 2004 10th Biennial Forest Service Remote Sensing Applications Conference. April 2004. Salt Lake City, UT.

Kaufman, Y.J., Setzer, A.W., Justice, C.O., Tucker, C.J., Pereira, M.C., and Fung, I. 1990. Remote sensing of biomass burning in the tropics. In J. G. Goldammer (Ed.), Fire and the tropical biota: ecosystem processes and global challenges (pp. 371– 399). Berlin: Springer-Verlag.

Kustas, W. P., and Norman, J. M. 2000. A two-source energy balance approach using directional radiometric temperature observations for sparse canopy covered surfaces. Agronomy Journal 92: 847–854.

Hernandez-Stefanoni, J.L. and Ponce-Hernandez, R. 2004. Mapping the spatial distribution of plant diversity indices in a tropical forest using multi-spectral satellite image classification and field measurements. Biodiver. Conserv. 13: 2599–2621.

Hoppus, M, . and Lister, A.J. 2005. Measuring forest area loss over time using FIA plots and satellite imagery. P. 91-97 in Proc. of the 2002 FIA syrnposium/annual meeting ofthe southern memurationists, November 19 -2 1, 2002, New Orleans, LA, USDA GTR NC-252.

Huang, C., Wylie, B., Yang, L., Homer, C., and Zylstra, G. 2000. Derivation of a Tasseled Cap Transformation based on Landsat 7 At-Satellite Reflectance. URL: ttp//landcover.usgs.gov/pdf/tasseled.pdf. Raytheon, ITSS, USGS EROS Data Center, Sioux Falls, South Dakota (last date accessed: 19 February 2004).
Hudak, A.T., and Brockett B.H., 2004a. Mapping fire scars in a southern African savannah using Landsat imagery. International Journal of Remote Sensing. 25, 3231 – 3243.

Hudak, A.T., Robichaud, P.R., Evans, J.B. 2004b. Field validation of burned area reflectance classification (BARC) products for post fire assessment. Proceedings of the 2004 10th Biennial Forest Service Remote Sensing Applications Conference. April 2004. Salt Lake City, UT.

Hunt, Jr., E.R., and Rock, B.N. 1989. Detection of changes in leaf water content using near- and middle-infrared reflectances. Remote Sensing of Environment, 30, 43–54.

Hyyppä, J., Hyyppä, H., Inkinen, M., Engdahl, M., Linko, S., and Zhu, Y-H. 2000. Accuracy comparison of various remote sensing data sources in the retrieval of forest stand attributes. Forest Ecology and Management, 128, pp, 109-120.

Jackson, R. D.1983. Spectral indices in n-space. Remote Sensing Environ. 13: 409-421.

Jensen, J.R. 1996. Introductory digital image processing. Upper Saddle River, NJ: Prentice Hall. 318 p.

Justice, C.O., Kendall, J.D., Dowty, P.R., and Scholes, R.J. 1996. Satellite remote sensing of fires during the SAFARI campaign using NOAA Advanced Very High Resolution Radiometer Data. J. Geophy. Res, 101:23851-23864.

Justice, C.O., Giglio, L., Korontzi, S., Owens, J., Morisette, J.T., Roy, D., Descloitres, J., Alleaume, S., Petitcolin, F., and Kaufman, Y. 2002. The MODIS fire products. Remote Sensing of Environment, 83, 245–263.

Kaufman, Y.J., and Justice, C. 1998. Algorithm Technical Background Document. MODIS fire products. (Version 2 .2 Nov. 10 1998) (EOS ID# 2741).

Kaufman, Y.J., Ichoku, C., Giglio, L., Krontzi S., Chu, D A., Hao, W.M., Li, R., and Justice, C.O. 2003. Fire and smoke observed from the Earth Observing System MODIS instrument-products, validation, and operational use. Int. J. Remote Sensing 24(8):1765-1781.

Kaufman, Y. J., Justice, C. O., Flynn, L. P., Kendall, J. D., Prins, E. M., Giglio, L., Ward, D. E., Menzel, W. P., and Setzer, A. W. 1998. Potential Global Fire Monitoring From EOS-MODIS. Journal of Geophyical Research, 103:32215-32238.

Kaufman, Y.J., Setzer, A.W., Justice, C.O., Tucker, C.J., Pereira, M.C., and Fung, I. 1990: Remote sensing of biomass burning in the tropics. In Goldammer, J.G., editor, Fire in the tropical biota.Berlin: Springer-Verlag, 400–17.

Kauth, R. J., and Thomas, G.S. 1976. The tasseled cap: a graphic description of the spectral–temporal development of agricultural crops as seen by Landsat. Pages 41–50 *in* Proceedings of the Symposium on Machine Processing of Remotely Sensed Data. Purdue University, West Lafayette, Indiana, USA.

Keane, R.E., Burgan, R., and van Wagtendok, J. 2001. Mapping wildland fuels for fire management across multiple scales: Integrating remote sensing, GIS, and biophysical modeling. International Journal of Wildland Fire. 10:301-319.

Keane, R.E., Mincemoyer, S.A, Schmidt, K.M., Long, D.G., and Garner, J.L. 2002. Mapping vegetation and fuels for fire management on the Gila National Forest Complex, New Mexico. General Technical Report. RMRSGTR-46- CD. Ogden, UT:

U.S. Department of Agriculture, Forest Service, Rocky Mountain Research Station. pp. 1-126.

Kennedy, P.J., Belward, A.S., and Gregoire, J.M. 1994. An improved approach to fire monitoring in West Africa using AVHRR data. Int. J. Remote Sensing, 15:2235-2255.

Kessell, S.R. 1979. Gradient Modeling: resource and fire management. Springer Verlag, New York, pp. 1-432.

Key, C.H. and Benson, N.C. 2002. Measuring and Remote sensing of burn severity. In J.L. Coffelt and R.K. Livingston, U.S. Geological Survey Wildland Fire Workshop, Los Alamos, NM October 31-November 3, 2000. USGS Open-File Report 02-11. pp 55.

Li, Y., Vodacek, A., Kremens, R.L., Ononye, A., and Tang, C., 2005. A Hybrid Contextual Approach to Wildland Fire Detection Using Multispectral Imagery," IEEE Transactions on Geoscience and Remote Sensing. September 2005, volume 43, number 9, pp 2115-2126.

Lieberman, A.R., Stow, D., Rogan, J., and Franklin, J. 2004. Mapping burn severity in southern California Mediterranean type vegetation using Landsat and IKONOS data. Proceedings of the 2004 10th Biennial Forest Service Remote Sensing Applications Conference. April 2004. Salt Lake City, UT.

Lu, D. 2006. The potential and challenge of remote sensing‐based biomass estimation. International Journal of Remote Sensing, 27, 7, 1297-1328

Moisen, G.G., Blackard, J.A., and Finco, M. 2004. Proceedings of the 2004 10th Biennial Forest Service Remote Sensing Applications Conference. April 2004. Salt Lake City, UT.

Morse, A., Tasumi, M., Allen, R.G., and Kramber, W.J. 2000. Final Report. Application of the SEBAL Methodology for Estimating Consumptive Use of Water and Streamflow Depletion in the Bear River Basin of Idaho through Remote Sensing. Idaho Department of Water Resources. University of Idaho, Department of Biological and Agricultural Engineering. Submitted to: The Raytheon Systems Company; Earth Observation System Data and Information System Project.

Nemani, R., Pierce, L., Running, S., and Band, L. 1993. Forest ecosystem processes at the watershed scale: sensitivity to remotely-sensed leaf area index estimates. Int. J. Remote Sensing, 14:2519–2534.

Ohmann, J.L. and Gregory, M.J., 2002. Predictive mapping of forest composition and structure with direct gradient analysis and nearest neighbor imputation in coastal Oregon, USA. Can. J. For. Res. 32, 725-741.

Opitz, D.W., Morris, M., and Blundell S. 2004. A change detection system for natural resource applications. Proceedings of the 2004 10th Biennial Forest Service Remote Sensing Applications Conference. April 2004. Salt Lake City, UT.

Puzzolo, V., De Natale, F., and Giannetti, F. 2003. Forest species discrimination in an alpine mountain area using a fuzzy classification of multi-temporal SPOT (HRV) data. Geoscience and Remote Sensing Symposium, 2003. IGARSS '03. Proceedings. 2003 IEEE International.4, 2538-2540.

Peña-barragán, J.M., López-granados, F., Jurado-expósito, M., and García-torres, L. 2006. Spectral discrimination of Ridolfia segetum and sunflower as affected by phenological stage. Weed Research. 46:1,10-21.

Pyne, S. J., Andrews, P.L., and Laven, R.D. 1996. Introduction to Wildland Fire. John Wiley and Sons Inc., New York, pp. 1-769.

Qi, J., Chehbouni, A., Huete, A.R., and Kerr, Y.H. 1994. Modified Soil Adjusted Vegetation Index (MSAVI), Remote Sensing of Environment 48: 119-126.
Riano, D., E. Meier, B. Allgower, E. Chuvieco, and S.L. Ustin. 2003. Modeling airborne laser scanning data for the spatial generation of critical forest parameters in fire behavior modeling. Remote Sensing of Environment 86:177-186.

Richardson, A.J. and Wiegand, C.L., 1977. Distinguishing vegetation from soil background information. Photogr. E. R.43: 1541-1552.

Rogan, J. and Yool, S.R. 2001. Mapping fire-induced vegetation depletion in the Peloncillo Mountains, Arizona and New Mexico. International Journal of Remote Sensing, 22(16), 3101– 3121.

Rouse, J.W., Haas, R.H., Deering, D.W. and Sehell, J.A. 1974. Monitoring the vernal advancement and retrogradation (Green wave effect) of natural vegetation. Final Rep. RSC 1978-4, Remote Sensing Center, Texas A&M Univ., College Station.

Rude, M. 2004. Communities at risk of wildfire on Alaska's Kenai Peninsula use remote sensing and mobile GIS tools on the ground. Proceedings of the 2004 10th Biennial Forest Service Remote Sensing Applications Conference. April 2004. Salt Lake City, UT.

Ruefenacht, B. 2004. Use of regression-trees in remote sensing. Proceedings of the 2004 10th Biennial Forest Service Remote Sensing Applications Conference. April 2004. Salt Lake City, UT.

Saatchi, S.S. and Rignot, E. 1997. Classification of Boreal forest cover types using SAR images. Remote Sensing of Environment 60, 270–81.

Sader, S., Hoppus, M., Metzler, J., and Jin, S. 2005. Perspectives of Maine Forest Cover Change from Landsat Imagery and Forest Inventory Analysis (FIA). Journal of Forestry. 103(6): 299-303.

Salvador, R., Valeriano, J. , Pons, X., and Díaz-Delgado, R. 2000. A semiautomatic methodology to detect fire scars in shrubs and evergreen forests with Landsat MSS time series. International Journal of Remote Sensing 21: 655–673.

Sims, D. A., and Gamon, J. A., 2003. Estimation of vegetation water content and photosynthetic tissue area from spectral reflectance: a comparison of indices based on liquid water and chlorophyll absorption features. Remote Sensing of Environment 84: 526-537.

Steininger, M.K., Tucker, C.J., Ersts, P., Killeen, T.J., Villegas, Z. and Hecht, S.B. 2001. Clearance and fragmentation of tropical deciduous forest in the Tierras Bajas, Santa Cruz, Bolivia. Conservation Biology 15, 856–66.

Toomey, M. and Vierling, L.A. 2005. Multispectral remote sensing of landscape level foliar moisture: techniques and applications for forest ecosystem monitoring. Can. J. For. Res. 35(5): 1087-1097.

TBRS, 2003. The Terrestrial Biophysics and Remote Sensing Lab, Soil, Water, and Environmental Science Department at the University of Arizona. http://tbrs.arizona.edu/project/MODIS/evi.php.

Tucker, C.J. 1979. Red and photographic infrared linear combinations for monitoring vegetation. Remote Sensing Environ. 8: 127-150.

Tucker, C.J. 1980. Remote sensing of leaf water content in the near infrared. Remote Sensing of Environment, 10, 23– 32. Proceedings of the 2004 10th Biennial Forest Service Remote Sensing Applications Conference. April 2004. Salt Lake City, UT.

Ufnar, D.R., Frazier, B.E., Busacca, A.J., Lammers, D., and Fisk, H. 2004. Updating landtype association map techniques in region 6 using the TEUI-geospatial tooolkit. Proceedings of the 2004 10th Biennial Forest Service Remote Sensing Applications Conference. April 2004. Salt Lake City, UT.

van Leeuwen, W.J.D and Geoff Sammons, 2003. Seasonal Land Degradation Risk Assessment for Arizona. Proceedings of the 30th International Symposium on Remote Sensing of Environment, Honolulu, Hawaii November 10-14, 2003.

van Leeuwen, W.J.D., Orr, B., Stuart E. Marsh, Grant Casady, Dan Tuttle, Laura Baker, Elisabeth vander Leeuw, Wolfgang Grunberg, Charles F., Hutchinson. 2004. The use of MODIS products in a geospatial decision support tool for rangeland monitoring. Proceedings of the 2004 10th Biennial Forest Service Remote Sensing Applications Conference. April 2004. Salt Lake City, UT.

Wang, J., Sammis, T.W., Meier, C.A., Simmons, L.J., Miller, D.R., and Samani, Z. 2005a. A modified SEBAL model for spatially estimating pecan consumptive water use for las cruces, new mexico. 15th Conference on Applied Climatology. Hilton Savannah DeSoto, Savannah, Georgia. 20-24 June, 2005.

Wang, J., Sammis, T.W., Meier, C.A., Simmons, L.J., Miller, D.R., and Bathke, D. 2005b. Remote Sensing Vegetation Recovery after Forest Fires using Energy Balance.

Sixth Symposium on Fire and Forest Meteorology Sponsored by American Meteorological Society Radisson Hotel Canmore, AB, Canada 25–27 October, 2005. Paper number 7.6.

Wright, R., Flynn, L., Garbeil, H., Harris, A., and Pilger, E. 2002. Automated volcanic eruption detection using MODIS. Remote Sensing of Environment, 82:135-155.

Table 1 Launch date, status, spatial and temporal resolutions of selected satellite sensors.

	Landsat 5 TM/7ETM+	ASTER	Spot 4[a]	Spot 5[a]	AVHRR	MODIS	ALI	Quickbird-2	IKONOS-2
Owner	NASA	NASA	Space Imaging company registered under French law	Space Imaging company	NOAA/NASA	NASA	NASA	DigitalGlobe, a company in the US	Space Imaging company
Launched Time	March 1984/ April 1999	December 1999	March 1998	May 2002	Since 1978 June 11, several satellite sensors have been launched.	Decmber1999, Terra satellite; April 2002, Aqua satellite.	November 2000	October 2001	September 1999
Status	Landsat 5 TM: after July 14, 1998, sensor malfunction. Landsat7 ETM+: the Scan Line Corrector aboard malfunctioned on May 31, 2003. Data only in the middle part of the images can be used.	Working	Working	Working	Recent launched sensors (2000, 2002, 2005) still work well. Continuous historical data from 1978 to present are available.	Terra MODIS band 5 and Aqua MODIS band 6 have erroneous data.	Working	Working	Working
Spatial Resolution (m)	15-120	15-90	20 (10 m monochromatic)	10 m (2.5-m panchromatic)	1100	250-1000	30 m (10-m Panchromatic)	0.6-2.44	1-4
Temporal Resolution (day)	16 [b]	16 [b]	3 [b]	3 [b]	1	1-2	16 [b]	1-3.5 [b]	1-3 [b]
Scene Size (km by km)	185 x 185	60 x 60	56 x 56	56 x 56	2400 x6400	2300 x 2300	37 x 185	16.5 x 16.5	11.3 x 11.3
Price for each achieved raw data scene (US $)	600	Free[c]	1200-1900	3375-6750	Free for raw L1B data; $190 for geo registered L1B.	Free	250-500	$22.5 /km^2, minimum 25 km^2	$7/km^2, minimum 49 km^2

[a]: There is an additional sensor Vegetation sensor on Spot 4 and 5 satellites which has a resolution of 1 km for the whole field of view of 2400 km, offering

almost daily coverage of the whole of the earth's surface. Of its 4 spectral bands, 3 bands characterize vegetation (0.61-0.68 μm red band, 0.78-0.89 μm near infrared, and 1.58-1.75 μm short wave infrared) and the fourth band (0.43-0.47 μm, blue) is for atmospheric correction.

(b): This is the potential temporal resolution for a location because the historical data may have not been available if nobody has requested that the satellite collects data on this date and location.

(c): The price of higher level products (such as temperature and reflectance) derived from the raw radiance data are $80 each scene. Only ASTER and MODIS provide higher level products.

Table 2. Spectral and spatial resolutions and principle application for Landsat 5 TM, Landsat 7 ETM+, ASTER, ALI, Quickbird-2, IKONOS-2, Spot and MODIS satellite sensors.

Spectral Resolution (μm)	Spectral Location	Spatial Resolution (m)								Principle Application [a]
		Landsat5 TM /7ETM+	ASTER	ALI	Quick bird-2	IKON OS-2	Spot 4/5	AVHRR	MODIS	
All: 0.45 – 0.52, except ALI: 0.43-0.453, 0.45-0.515, MODIS: 0.459-0.47	B[b]	30/30	N/A[c]	30	2.44	4	N/A	N/A	500	Costal water mapping Soil vegetation differentiation Deciduous/Coniferous differentiation
All: 0.52 – 0.60, except ALI: 0.525-0.605, Spot: 0.5-0.59, MODIS:0.545-0.56	G	30/30	15	30	2.44	4	20/10	N/A	500	Green reflectance by healthy vegetation
All: 0.63 – 0.69, except Spot: 0.61-0.68; AVHRR:0.58-0.68	R	30/30	15	30	2.44	4	20/10	1100	250	Chlorophyll absorption for plant species differentiation Forest vigor
All: 0.76 – 0.90, except ASTER: 0.78-0.86, ALI: 0.775-0.805, 0.845-.89, Quickbird-2: 0.76-0.89 Spot: 0.79-0.9, MODIS: 0.841-0.87, AVHRR:0.725-1.10	NIR	30/30	15	30	2.44	4	20/10	1100	250	Biomass surveys Water body delineation Forest vigor
1.23-1.25 MODIS only	SWIR	N/A	N/A	N/A	N/A	N/A	N/A	N/A	500	Leaf area index, land and vegetation classification
All: 1.55 – 1.75, except ASTER : 1.6-1.7, Spot: 1.58-1.75, MODIS: 1.628-1.652, AVHRR:1.58-1.64, Daytime only, available for AVHRR	SWIR	30/30	30	30	N/A	N/A	20/20	1100	500	Vegetation moisture measurement Snow cloud differentiation

14-16 (After 1998-05-13)										
All: 2.08 – 2.35, except ASTER: 1.45-2.185, 2.185-2.225, 2.235-2.285, 2.295-2.365, 2.36-2.43 MODIS: 2.105-2.155, AVHRR: 3.55-3.93	SWIR	30/30	30	30	N/A	N/A	N/A	1100	500	Hydrothermal mapping
All: 10.4 – 12.5, except ASTER: two bands 10.25-10.95, 10.95-11.65, AVHRR: two bands 10.30-11.30, 11.50-12.50	TIR	120/60	90	N/A	N/A	N/A	N/A	1100	See note[(d)]	Plant heat stress measurement Other thermal mapping
All: 0.52 – 0.90, except ASTER: 0.52-0.6, Quickbird-2: 0.45-0.9, IKONOS-2: 0.526-0.929, Spot4: 0.61-0.68, Spot5: 0.48-0.71	All: Pan chromatic, G – NIR, except ASTER: G; Quickbird-2: B- NIR, Spot4: R.	N/A/15	15	10	0.61	1	10/2.5	1100	N/A	Vegetation mapping

Website:
Landsat: landsat7.usgs.gov, ASTER: http://lpdaac.usgs.gov/aster/asterdataprod.asp, ALI: eo1.gsfc.nasa.gov/Technology/ALIhome1.htm, Quickbird-2: http://www.digitalglobe.com/, IKONOS-2: http://www.spaceimaging.com, Spot: www.spot.com, AVHRR: http://edc.usgs.gov/products/satellite/avhrr.html#description, MODIS: modis.gsfc.nasa.gov

[(a):] The principle applications was concluded by Nicholas M. Short, Sr. (http://rst.gsfc.nasa.gov/Intro/Part2_20.html).
[(b):] B: blue, G: green, R: red, NIR: near infrared, SWIR: short wave infrared.
[(c):] N/A: Not available.
[(d):] MODIS has additional 29 bands from 0.405 to14.385 μm which include 16 thermal infrared bands from 3.66 to 14.385 μm.

Table 3. Selected indices and their definition used in remote sensing for forest health.

Index name	Acronym	Index property	Definition [(a)]	Reference
Normalized Difference Vegetation Index	NDVI	Vegetation index	$\frac{\alpha_{\mathrm{NIR}} - \alpha_{\mathrm{R}}}{\alpha_{\mathrm{NIR}} + \alpha_{\mathrm{R}}}$	Falkowski et al., 2005
Simple Ratio	SR	Vegetation index	$\frac{\alpha_{\mathrm{NIR}}}{\alpha_{\mathrm{R}}}$	Falkowski et al., 2005
Green-red ratio	GRVI	Vegetation index	$\frac{\alpha_{\mathrm{G}} - \alpha_{\mathrm{R}}}{\alpha_{\mathrm{G}} - \alpha_{\mathrm{R}}}$	Falkowski et al., 2005
Modified Soil Adjusted Vegetation Index	MSAVI	Vegetation index	$\frac{\alpha_{NIR} - \alpha_{R}}{\alpha_{NIR} + \alpha_{R} + L}(1+L)$	Qi et al., 1994
Enhanced vegetation index	EVI	Vegetation index	$G \times \frac{\alpha_{NIR} - \alpha_{R}}{\alpha_{NIR} + c_1\alpha_{R} - c_2\alpha_{B} + l}$	TBRS, 2003
Foliar moisture index	MI1	Foliar moisture index	$\frac{\alpha_{\mathrm{NIR}}}{\alpha_{\mathrm{R}}\alpha_{SWIR}}$	Toomey and Vierling, 2005
Foliar moisture index	MI2	Foliar moisture index	$\frac{\alpha_{\mathrm{NIR}} - \alpha_{\mathrm{R}}}{(\alpha_{\mathrm{NIR}} + \alpha_{\mathrm{R}}) \times \alpha_{SWIR}}$	Toomey and Vierling, 2005
Foliar moisture index	MI3	Foliar moisture index	$\frac{2.5(\alpha_{\mathrm{NIR}} - \alpha_{\mathrm{R}})}{(1 + \alpha_{\mathrm{NIR}} + 6\alpha_{\mathrm{R}} - 7.5\alpha_{\mathrm{B}}) \times \alpha_{SWIR}}$	Toomey and Vierling, 2005
Infrared ratio index	IRI	Foliar moisture index	$\frac{\alpha_{\mathrm{NIR}}}{\alpha_{SWIR}}$	Toomey and Vierling, 2005
Normalized Difference Infrared Index,	NDII	Foliar moisture index	$\frac{\alpha_{\mathrm{NIR}} - \alpha_{SWIR}}{\alpha_{\mathrm{NIR}} + \alpha_{SWIR}}$	Toomey and Vierling, 2005
wide band Normalized Difference Infrared Index	wNDII	Foliar moisture index	$\frac{2\alpha_{\mathrm{NIR}} - \alpha_{SWIR}}{2\alpha_{\mathrm{NIR}} + \alpha_{SWIR}}$	Toomey and Vierling, 2005
Global Vegetation Moisture Index	GVMI	Foliar moisture index	$\frac{(\alpha_{NIR} + 0.1) - (\alpha_{SWIR} + 0.02)}{(\alpha_{NIR} + 0.1) + (\alpha_{SWIR} + 0.02)}$	Ceccato et al., 2002 a ,b
Normalized Burn Ratio	NBR	Burn index	$\frac{\alpha_{\mathrm{NIR}} - \alpha_{SWIR}}{\alpha_{\mathrm{NIR}} + \alpha_{SWIR}}$	Cocke et al., 2005
Background (not burnt) ratio	BR	Burn index	$\frac{\alpha_{G} - \alpha_{TIR}}{\alpha_{G} + \alpha_{TIR}}$	Li et al., 2005
NBR change index	dNBR	Burn index	$NBR_{Before} - NBR_{After}$	Cocke et al., 2005
Normalized Thermal Index	NTI	Burn index	$\frac{R_{3.9} - R_{12}}{R_{3.9} + R_{12}}$	Wright et al., 2002

[(a)] α_{NIR} is the reflectance of near infrared band, α_{R} is the reflectance of red band,

α_G is the reflectance of green band, α_B is the reflectance of blue band, and α_{SWIR} is the reflectance of short wave infrared band, and α_{TIR} is the reflectance of thermal infrared band.

L is a correction factor which ranges from 0 for very high vegetation cover to 1 for very low vegetation cover.

C1: atmosphere resistance red correction coefficient,

C2: atmosphere resistance blue correction coefficient,

l: canopy background brightness correction factor,

G: gain factor.

where the coefficients adopted in the EVI algorithm are, l=1, C1 = 6, C2 = 7.5, and G (gain factor) = 2.5 (TBRS, 2003).

NBR_{Before} and NBR_{After} are NBR values before and after fires.

$R_{3.9}$ is the radiance of 3.9 μm band and R_{12} is the radiance of 12 μm band.

Table 4. Selected studies of satellite remote sensing for forest health. The satellite, band and parameter used, method, and accuracy are provided. (R: red, G: green, B: blue, NIR: near infrared, SWIR: short wave infrared, TCT: Tasseled Cap Transformation, PCA: Principle Component Analysis.).

Study/ Reference	Satellite/Band/parameter	Method	Accuracy
Fuel mapping Falkowski et al., 2005	ASTER / NIR, R, G / NDVI, GRVI, SR	Regression and gradient model	R^2>77% for canopy closure prediction, R^2>46% for bulk density prediction, The prediction of potential vegetation type agreed with the local expert system.
Fuel mapping Rollins et al., 2005	Landsat 5 / R, G, B, NIR, SWIR / PCA components 1 , 2, and 3; Brightness, Wet and Greeness of TCT, LAI, MNDVI	Regression and gradient modeling.	For fuel load prediction (kg/m^2) Accuracy from 51%-85%.
Foliar moisture stress Toomey and Vierling, 2005	Landsat 5 TM, ASTER / R, G, B, NIR, SWIR /NDVI, SR, MI1, MI2, MI3, IR, wNDII, PCA, and TCT	Regression	Correlation coefficients with SMC, PCA second component: R^2=0.765, wNDII: R^2=0.627, TCT wetness: R^2=0.638, R^2 for others R^2 are around 0.5-0.6.
Fire detection Justice et al., 2002	MODIS /TIR bands: 3.66-4.08 μm, 3.929-3.989μm, 11.770-12.270 μm, NIR 0.86 μm /temperature, reflectance	Contextual and threshold algorithms	The detection algorithm is currently functioning reasonably well. Some sensitivity to relatively small yet obvious fires has been sacrificed to reduce persistent false detections occurring in regions of hot, reflective exposed soil. Nevertheless, some of these persistent false alarms remain.
Fire detection Li et al., 2005	MODIS /250-m red and NIR, four TIR bands from 3.66-4.08 μm, one 11.770-12.270 μm TIR /BR, temperature	Hybrid algorithm	The new hybrid algorithm works well and yielding very few, if any, false alerts.
Post-fire burn area and severity mapping Hudak et al., 2004b	Landsat 5, Spot4, ASTER, MODIS /NIR SWIR, R / NBR, dNBR, NDVI	Regression	Correlation between the satellite parameters and burned severity R^2: 44-79%
Post-fire burn area and severity mapping Fraser and Li, 2002	Spot Vegetation / NIR, SWIR / NBR, NDVI	Spectral change detection	>85%
Post-fire burn area and	Landsat 7 ETM+	Compare the BNR difference	73%

severity mapping Cocke et al., 2005	/ NIR SWIR / dBNR	before and after fires	
Vegetation classification/ Hoppus and Lister, 2005	Landsat / R, G, B, NIR, SWIR, TIR /NDVI, PCA, TCT	Unsupervised and supervised algorithms	The forest/nonforest estimates are in close agreement with the FIA data.
Vegetation classification/ Sader et al., 2005	Landsat/ R, G, B, NIR, SWIR, TIR / N/A	Unsupervised algorithm and visual interpretation	The forest/nonforest accuracy was 83%. The accuracy of no change forest, forest loss, and forest gain were 90, 88, and 92%, respectively
Vegetation classification Steininger et al., 2001	Landsat5/R, NIR, SWIR/spectral signature	Supervised spectral classification	75%-98%
Landscape mapping Ruefenacht, 2004	Landsat / NIR SWIR, R, G, B / Spectral signature	Regression-trees	Percent canopy average relative error was 55%, Percent impervious surface cover analysis had an average error of 36%. The overall accuracy of this classification was 99% got classifying forest, non-forest, mixed, and water.
Landscape mapping Hernandez-Stefanoni and Ponce-Hernandez, 2004	Landsat 7 / NIR SWIR, R / N/A	Supervised classification	82%
Insect infestation Rude, 2004	Landsat7 / NIR SWIR, R, G, B / N/A	Supervised classification	It did an adequate evaluation of very broad categories of deciduous, coniferous, and mixed forests. But it did not tell where the dead trees are which were infested by spruce bark beetles.
Forest type mapping Puzzolo et al., 2003	Spot / NIR SWIR, R / N/A	Supervised classification	79-86%.
Forest type mapping Ohmann and Gregory, 2002	Landsat 5 / NIR SWIR, R, G, B /TCT wetness, brightness, greenness	Gradient modeling using inputs of TCT components, climate, topography, forest ownership, Geology, Location.	56-89% for the prediction of seven species.
Invasive weed detection Peña-barragán et al., 2006	Quickbird-2, IKONOS-2 / B, G, R, NIR /NDVI, otehr reflectance ratios of G, R, NIR	Analysis of variance	The values of NDVI and other indices of Ridolfia segetum were significantly different from the values of bare soil, sunflowers.

Forest vigor Beck and Gessler, 2004	Landsat7 / R, G, B, NIR, SWIR / NDVI, TCT wetness and greenness	change detection of the indices	Show high potential for efficiently mapping and monitoring vegetation change in a cost-effective manner.
Biomass Foody et al., 2003	Landsat/ R, G, B, NIR, SWIR / NDVI, other ratios of different bands	Regression, Neural networks	R^2>50%
Stand volume Hyyppä et al., 2000	Spot and Landsat /all bands /TCT, NDVI, band ratios	Regression	R^2>31%-44%
Land degradation model van Leeuwen and Sammons, 2003	MODIS / NIR, R / NDVI	Integrated MODIS vegetation index time series data and the spatially detailed climate data to predict soil loss and erosion	No ground truth comparison.

Table 5. Selected satellite data formats and software tools to read the data

Foramat	GeoTIFF	HDF	Fast	NDF	NITF
Reader tools	ArcView Extension: TIFF 6.0 Image Support6, ENVI, SOCET GXP v2.2, DRG/GeoTIFF viewer (free software), PCI Freeware Viewer (free software) Software tool list: http://home.earthlink.net/~ritter/geotiff/software.html	ENVI, Cube Visualization, Global Mapper v6.06, HDFView (free software), McIDAS-Lite (free software) Software tool list: http://hdf.ncsa.uiuc.edu/hdfeoss.html	ENVI, dlgv32 Pro, SOCET GXP v2.2	ENVI, SOCET GXP v2.2	ArcView Extension: NITF Image Support6, SOCET GXP v2.2
Landsat 1, 2, 3 , 4 and 5	x (for Landsat 5 TM data only)			x	
Landsat 7 ETM+	x	x	x	x	
ASTER		x			
Spot 4 [(a)]					
Spot 5 [(a)]					
AVHRR					x
MODIS	x (some data products only)	x			
ALI		x			
Quickbird-2	x				x
IKONOS-2	x				x

(a): SPOT 4: CAP format; SPOT 5: DIMAP format. SOCET GXP v2.2 and ENVI can read these formats.

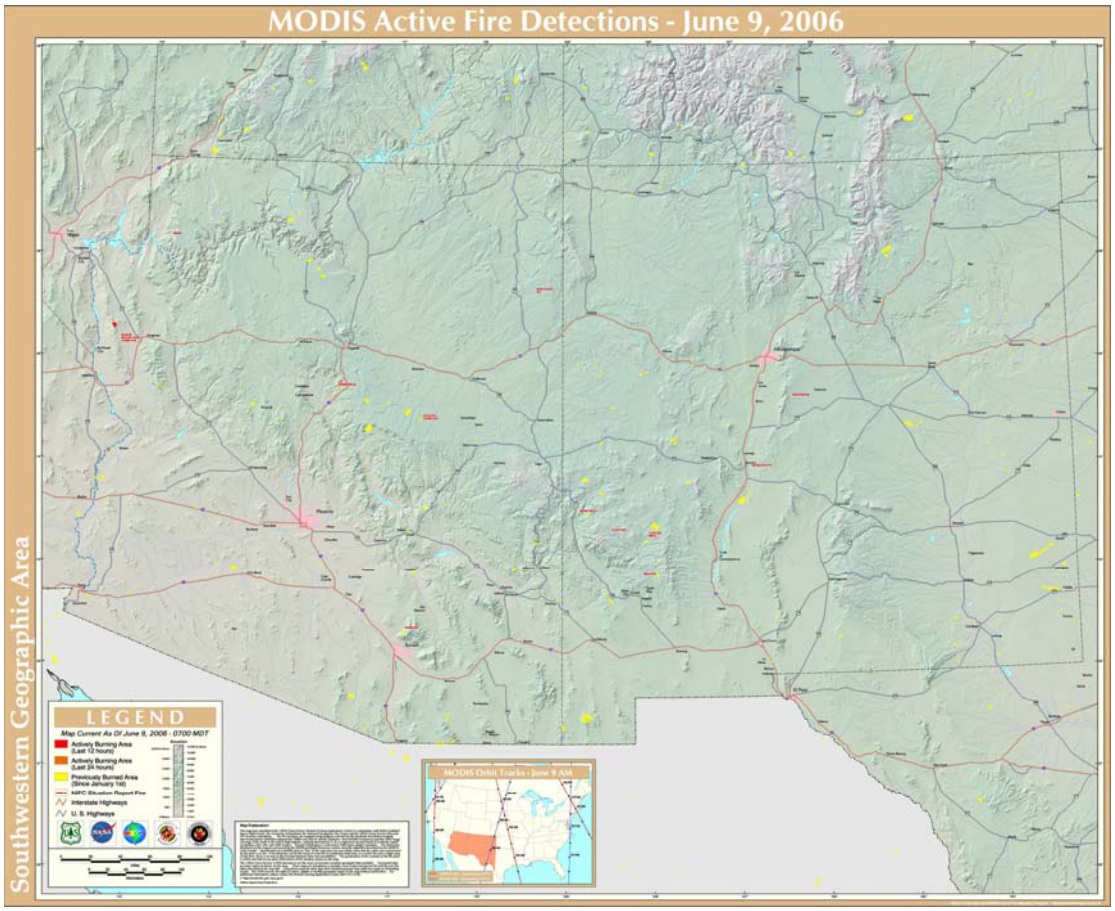

Figure1. A sample MODIS Active Fire Detection map for southwestern US on June 9, 2006. It was downloaded at the FSGeodata Clearinghouse at USDA Forest Service (http://svinetfc4.fs.fed.us/).

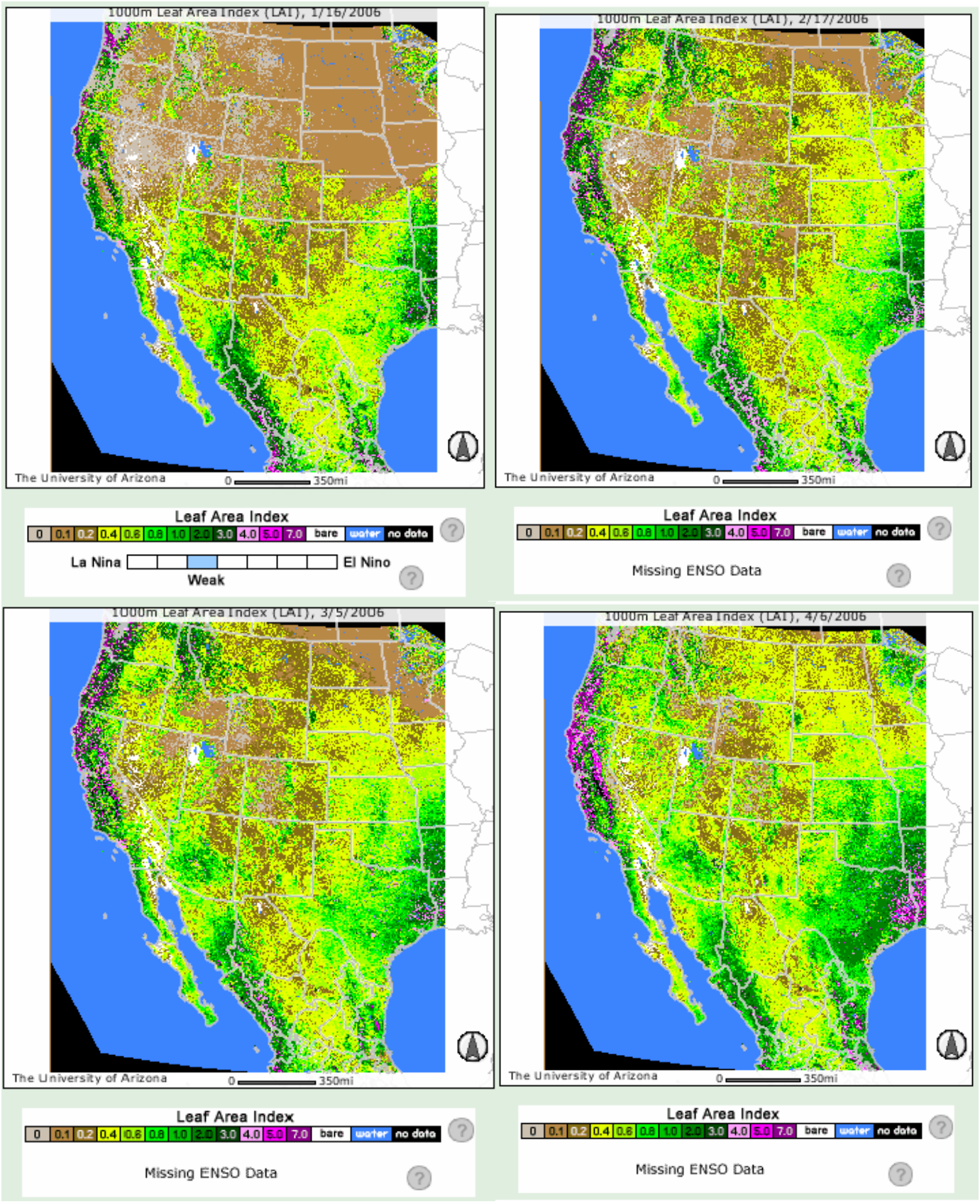

Figure 2. Western US LAI maps in January (top left), February (top right), March (bottom left), and April (bottom right) of 2006. The pictures were downloaded from Arizona Remote Sensing Center, Office of Arid Lands Studies, University of Arizona (http://rangeview.arizona.edu).